Full Paper: Oriented smectic-C* elastomers have been made by performing radical photo-crosslinking reactions in a polar state of the ferroelectric phase. This paper aims at the evaluation of structure-property-relationships. Two polymer systems – varying in the length of the mesogens, the ferroelectric polarization and the amount of crosslinkable groups – were synthesized. The ferroelectric properties of the resulting elastomers were studied using electro-optical investigations. The crosslinking of ferroelectric polysiloxanes with a modest polarization (50–105 nC/cm^2) and 15 or 25 mol-% of crosslinkable groups leads to polar elastomers, which can no longer be switched completely (voltages up to 400 V are not enough to reach the second, destabilized switching state). Ferroelectric polysiloxanes with a higher polarization (90–150 nC/cm^2) lead to elastomers, which can be switched again completely. This happens because the torque ($P_s \cdot E$) acting on the liquid crystalline director is – this time – large enough to overcome the elastic field of the polymer network.

Ferroelectric liquid crystalline elastomers, 2[a] Variation of mesogens and network density

*Elisabeth Gebhard, Rudolf Zentel**

Department of Chemistry and Institute of Materials Science, University of Wuppertal, Gaußstraße 20, D-42097 Wuppertal, Germany

(Received: April 27, 1999; revised: October 21, 1999)

1. Introduction

Slightly crosslinked liquid crystalline (LC) polymers that combine the properties of liquid crystalline phases (e.g. the self-organization of mesogens) and the elastic properties and formstability of polymeric networks are known as "liquid crystalline elastomers"[1–3]. Especially smectic-C* elastomers and smectic-C* networks are of widespread interest as they show remarkable electromechanical effects like piezoelectricity. Our approach to create smectic-C* elastomers starts with an orientation of photo-crosslinkable ferroelectric polymers in the electric field. In a second step the stabilization of one ferroelectric switching state is managed by UV-irradiation that transfers the smectic-C* polymer into a smectic-C* elastomer[4,5]. The preceeding paper[6] discusses the influence of the network topology and the orientation during crosslinking on the elastomer properties. This paper deals with the influence of modifications of the mesogens with respect to the size of the polarization and network density. This investigation is performed on systems with a preference for inter layer crosslinking[6], because here the coupling between the polymer network and the director orientation is strongest. To exclude H-bonding, acrylates instead of acrylamides[4] were used for crosslinking. The crosslinking density in the resulting elastomeric systems is varied by incorporating different amounts of photo-crosslinkable acrylate groups into the precursor ferroelectric terpolymers. The aim is to build up networks with a stable polar orientation in the liquid crystalline phases while the reorientation of the polar axis in alternating electric fields is still retained.

[a] Part 1: cf. ref.[6]

2. Experimental part

2.1 Synthesis

The syntheses of the ferroelectric copolysiloxanes and the photo-crosslinkable terpolysiloxanes are illustrated in detail in Scheme 1. Whereas the synthetic route to the ferroelectric copolysiloxanes was achieved by a single one-step hydrosilylation reaction connecting the low molar mass chiral mesogens to the copolysiloxane backbone (Scheme 1a), the crosslinkable terpolysiloxanes have to be synthesized using three polymer-analogous reactions (Scheme 1b). Our experiments showed that the hydrosilylation of mesogens containing both an olefinic double-bond and a crosslinkable acrylate or acrylamide group does not proceed in a definite and reproducible way. Therefore a protected mesogen with olefinic double bond was hydrosilylated to a copolysiloxane backbone in a first step. After the deprotection the polymers were functionalized in a DCC-esterification using a chiral and a crosslinkable acid[4].

The molecular structures and the synthetic route to the crosslinkable terpolymers **P2**–**P4** and **P6**–**P8** are given in Scheme 2 and Scheme 3. The OH-functionalized polymer **3**

  1022-1352/2000/0805–0911$17.50+.50/0

Scheme 1: Schematic synthetic routes to a) the ferroelectric copolysiloxanes via hydrosilylation reaction and b) the photo-crosslinkable terpolysiloxanes via three polymer-analogous reactions

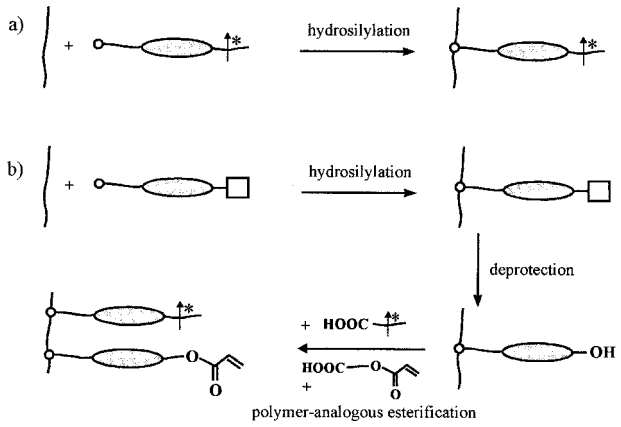

was prepared in analogy to ref.[4,7] Poly[(methylhydrogen-*co*-dimethyl)siloxane] in the ratio of 1:1.5 was obtained from ABCR (P_n = 27, P_w = 38; measured against PDMS, solvent toluene). In a classical hydrosilylation reaction using $[Pt(C_{10}H_{12})Cl_2]$ as catalyst the acetyl protected mesogen 4-(undec-10-enyloxy)-4′acetoxybiphenyl **(1)** was connected to the copolysiloxane backbone[7]. Cleaving the protecting group in compound **3** by hydrazinolysis resulted in the polysiloxane with free phenolic OH-groups (**3**)[4]. The catalyst *N*,*N*′-dimethylaminopyridine was changed to 4-pyrrolidinopyridine in the final esterification due to higher reactivity[8]. To synthesize the terpolymers **P2**–**P4** (2S, 3S)-2-chloro-3-methylpentanoic acid **(4)**[9] and 2-acryloyloxyethyl glutaric acid monoester **(5)** (synthesis described in 2.2.1.) in the presence of *N*,*N*′-dicyclohexylcarbodiimide (DCC) and 4-pyrrolidinopyridine were used to esterify the hydroxy groups quantitatively. 3-Nitro-4-(1-(S)-methylheptyloxy)benzoic acid **(6)**[7,10] and 4-(6-(acryloyloxyhexyloxy)benzoic acid **(7)**[11] were alternatively used to create the terpolymers **P6**–**P8**. In a typical run the OH-functionalized polymer **3** (exact

Scheme 2: Synthesis of terpolymers **P2**–**P4**

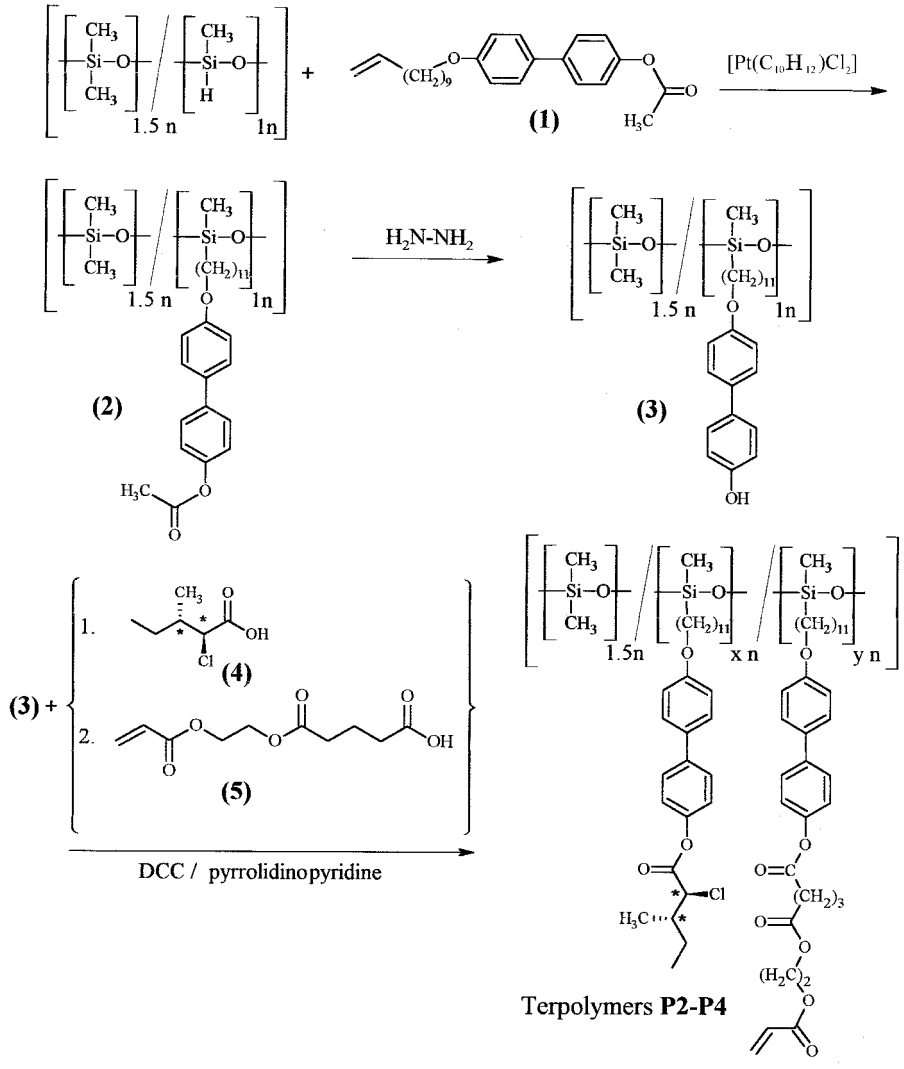

Scheme 3: Synthesis of terpolymers **P6**–**P8**

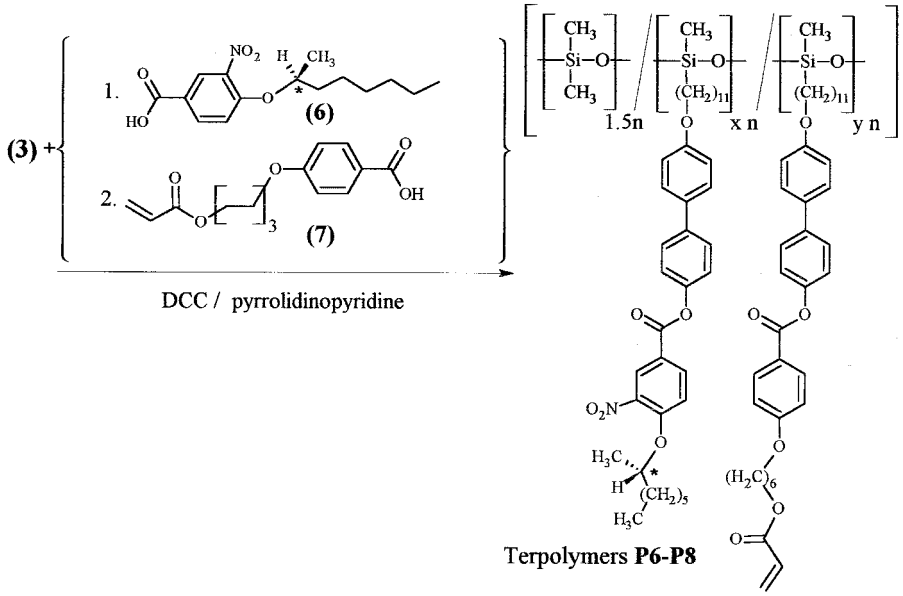

quantities used are given in 2.2) was dissolved in about 20 ml of dry tetrahydrofuran. After addition of the chiral acid and the first portion of 4-pyrrolidinopyridine the reaction mixture was cooled to 0 °C. A solution of the first portion of *N,N′*-dicyclohexylcarbodiimide (DCC) in a few millilitres of dry dichloromethane was added while the mixture was stirred. After three hours stirring at 0 °C the reaction mixture was allowed to warm to room-temperature over night. At this step the amount of esterified OH-groups was checked by IR spectroscopy. The remaining OH-groups were esterified with crosslinkable acid. Therefore the crosslinkable acid and the second portion of 4-pyrrolidinopyridine were added to the reaction mixture. The procedure described above is repeated using the second portion of *N,N′*-dicyclohexylcarbodiimide (DCC). A completely successful esterification of the OH-groups was checked. The cyclohexylurea was filtered off, the solvent was evaporated to a few millilitres volume and the polymer was precipitated from cold methanol. To purify the resulting polymer a chromatography using Al_2O_3 (neutral) and two further reprecipitations from methanol follow after the synthesis according to ref.[4)]

The synthesis of the chiral mesogens terminated by olefinic double bonds and typical hydrosilylation reactions to prepare copolymers **P1** and **P5** were carried out as described previously[12, 13)].

Tab. 1. Characterization of copolysiloxane **P1** and terpolysiloxanes **P2**–**P4**

System	Ratio (x:y)	Phase transitions (°C) without initiator	s_C^*/s_A-phase transition (°C) with 1 wt.-% initiator
P1	(1:0)	s_X 40/41 s_C*82 s_A 101 i	–
P2	(0.95:0.05)	s_X 33/34 s_C*77 s_A 101 i	s_C* 73/74 s_A
P3	(0.85:0.15)	s_X 33 s_C*75 s_A 101 i	s_C* 72 s_A
P4	(0.75:0.25)	s_X 33 s_C*78 s_A 103 i	s_C* 74 s_A

Tab. 2. Characterization of copolysiloxane **P5** and terpolysiloxanes **P6**–**P8**

System	Ratio (x:y)	Phase transitions (°C) without initiator	s_C^*/s_A-phase transition (°C) with 1 wt.-% initiator
P5	(1:0)	g 3 s_X 38 s_C*98 s_A 138 i	–
P6	(0.95:0.05)	g 9 s_X 31 s_C*115 s_A 155 i	s_C* 110 s_A
P7	(0.85:0.15)	g 8 s_X 32 s_C*116 s_A 152 i	s_c* 114 s_A
P8	(0.75:0.25)	g10 s_X 42 s_C*130 s_A 165 i	s_c* 128 s_A

2.2 Analytical data

The structures of the resulting polymers were checked by ^{1}H NMR spectroscopy. IR spectra were recorded to confirm that the hydroxy groups were almost quantitatively esterified by the acids (>95%) in the DCC-esterifications.

2.2.1 Synthesis of acryloyloxyethyl glutaric acid monoester (**5**)

11.4 g (0.1 mol) glutaric anhydride, 11.6 g (0.1 mol) 2-hydroxyethyl acrylic acid ester and one drop H_2SO_4 were mixed and stirred for 2 h at 50–60 °C. After cooling the reaction mixture was poured into 120 ml ice water. The organic phase is separated, the water phase is twice extracted with diethyl ether. The organic phases were dried over Na_2SO_4. The solvent was evaporated and the yellow-brown oil was fractionated in vacuum after addition of *p*-(2,6-di-*tert*-butyl)-cresol as stabilisator.

Yield: 9 g (39% of theory); clear, high viscous liquid. b.p. 155 °C ($5 \cdot 10^{-3}$ mbar).

^{1}H NMR (200 MHz, $CDCl_3$): δ = 10.45 (s, 1H, COOH), 6.43–6.34 (d, 1H, CH_2=CH-trans), 6.15–6.0 (m, 1H, CH_2=CH), 5.85–5.78 (d, 1H, CH_2=CH-cis), 4.35–4.15 (m, 4H, COO—CH_2—CH_2—OOC), 2.54–2.33 (m, 4H, ROOC—CH_2—CH_2—CH_2—COOH), 1.97–1.85 (m, 2H, ROOC—CH_2—CH_2—CH_2—COOH).

^{13}C NMR (100 MHz, $CDCl_3$): δ = 178.6 (COOH), 167.3 (OOC—CH_2), 165.6 (CH_2=CH—COO), 131.2 (CH_2=CH), 127.6 (CH_2=CH), 61.9 (CH_2=CH—COO—CH_2—CH_2—O), 32.65–32.59 (OOC—CH_2—CH_2—CH_2—COOH), 19.4 (OOC—CH_2—CH_2—CH_2—COOH).

IR (NaCl): 3250–3100 (OH), 2960 (C—H-Valence), 1730 (C=O-Valence), 1636 (C=C), 1412, 1298, 1188, 810 cm^{-1}.

2.2.2 Polymer **P1**

^{1}H NMR (200 MHz, $CDCl_3$): δ = 7.53–7.42 (m, 4H, aromat. H_2, H_6, $H_{2'}$, $H_{6'}$), 7.14–7.10 (d, 2H, aromat. H_3, H_5), 6.94–6.89 (d, 2H, aromat. $H_{3'}$, $H_{5'}$), 4.38–4.35 (C*H—Cl), 4.0–3.85 (m, 2H, CH_2—O), 2.35–2.1 (m, 1H, C*H—CH_3), 1.9–1.2 (m, 20H, CH_2), 1.18–1.05 (d, 3H, C*H—CH_3), 1.05–0.9 (t, 3H, CH_2—CH_3), 0.6–0.4 (s, 2H, Si—CH_2), 0.2–0 (m, 12H, Si—CH_3).

IR (film on NaCl): = 2962, 2924, 2878, 2854 (C—H valence), 1764 (C=O valence), 1608, 1498, 1466, 1290, 1260, 1096, 1026, 804 cm^{-1}.

Yield: 62% of theory.

$\overline{M}_n$ = 6400 g/mol, $\overline{M}_w$ = 8800 g/mol.

$[\alpha]_D^{21}$ = (–1.53)°, c = 0.015 g/ml in $CHCl_3$.

^{1}H NMR spectra of the polymers **P2**–**P4** are interpreted with the assignment of the H atoms shown in Fig. 1.

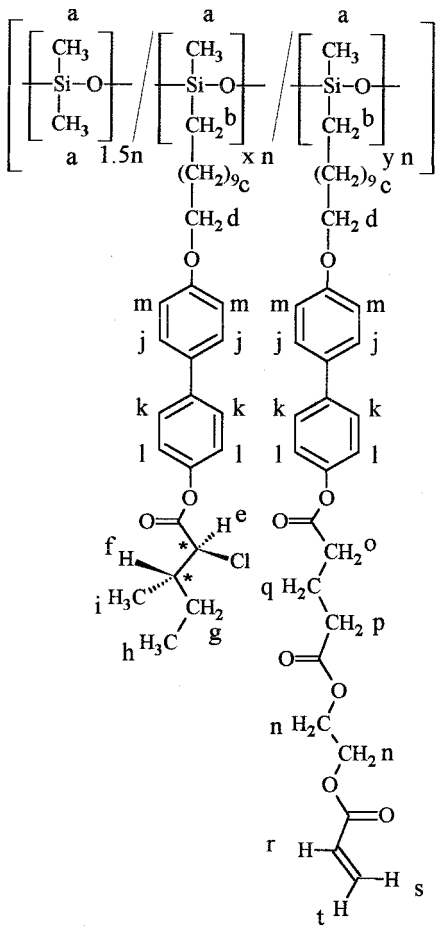

Fig. 1. Molecular structure of terpolymers **P2**–**P4** with assignment of H-atoms

2.2.3 Polymer **P2**

(x:y) = (0.95:0.05) quantities used:

890 mg (1.75 mmol) OH-functionalized polysiloxane **(3)**

342 mg (2.275 mmol, 1.3fold excess) (2S, 3S)-2-chloro-3-methylpentanoic acid **(4)**

34 mg (0.2275 mmol) 4-pyrrolidino-pyridine

470 mg (2.275 mmol) *N*,*N*′-dicyclohexylcarbodiimide (DCC)

161 mg (0.7 mmol, 0.4fold excess) 2-acryloyloxyethyl glutaric acid monoester **(5)**

10.5 mg (0.07 mmol) 4-pyrrolidinopyridine

145 mg (0.7 mmol) *N*,*N*′-dicyclohexylcarbodiimide (DCC)

^{1}H NMR (200 MHz, $CDCl_3$): δ = 7.49–7.41 (m, 4H, aromat. j, k), 7.13–7.09 (d, 2H, aromat. l), 6.93–6.89 (d, 2H, aromat. m), 6.46–6.27 (d, 0.05H, s), 6.18–6.04 (m, 0.05H, r), 5.89–5.85 (d, 0.05H, t), 4.51–4.29 (m, 1.15H, e + n), 3.93–3.14 (s, 2H, d), 2.64–2.44 (2m, 0.3H, o + p, q), 2.3–2.03 (m, 0.95H, f), 1.96–1.26 (m, 19.9H, c + g), 1.13–1.10 (d, 2.85H, i), 1.05–0.85 (t, 2.85H, h), 0.48 (s, 2H, b), 0.35–0 (m, 12H, a)

Yield: 71% of theory.

$\overline{M}_n$ = 7000 g/mol, $\overline{M}_w$ = 9400 g/mol.

$[\alpha]_D^{21}$ = (–1.532)°, c = 0.015 g/ml in $CHCl_3$.

2.2.4 Polymer **P3**

(x:y) = (0.85:0.15) quantities used:

750 mg (1.47 mmol) OH-functionalized polysiloxane **(3)**

255 mg (1.69 mmol, 1.15fold excess) (2S, 3S)-2-chloro-3-methylpentanoic acid **(4)**

25 mg (0.169 mmol) 4-pyrrolidino-pyridine

350 mg (1.69 mmol) *N*,*N*′-dicyclohexylcarbodiimide (DCC)

135 mg (0.588 mmol, 0.4fold excess) 2-acryloyloxyethyl glutaric acid monoester **(5)**

9 mg (0.0588 mmol) 4-pyrrolidinopyridine

122 mg (0.588 mmol) *N*,*N*′-dicyclohexylcarbodiimide (DCC)

^{1}H NMR (200 MHz, $CDCl_3$): δ = 7.46–7.41 (m, 4H, aromat. j, k), 7.13–7.09 (d, 2H, aromat. l), 6.93–6.89 (d, 2H, aromat. m), 6.50–6.27 (d, 0.15H, s), 6.18–6.05 (m, 0.15H, r), 5.86–5.81 (d, 0.15H, t), 4.45–4.24 (m, 1.4H, e + n), 3.93–3.18 (s, 2H, d), 2.64–2.45 (2m, 0.9H, o + p, q), 2.3–2.03 (m, 0.85H, f), 1.96–1.26 (m, 19.7H, c + g), 1.13–1.10 (d, 2.55H, i), 1.05–0.85 (t, 2.55H, h), 0.48 (s, 2H, b), 0.35–0 (m, 12H, a).

Yield: 67% of theory.

$\overline{M}_n$ = 7600 g/mol, $\overline{M}_w$ = 11100 g/mol.

$[\alpha]_D^{21}$ = (–1.274)°, c = 0.0149 g/ml in $CHCl_3$.

2.2.5 Polymer **P4**

(x:y) = (0.75:0.25) quantities used:

750 mg (1.47 mmol) OH-functionalized polysiloxane **(3)**

232 mg (1.54 mmol, 1.05fold excess) (2S, 3S)-2-chloro-3-methylpentanoic acid **(4)**

23 mg (0.154 mmol) 4-pyrrolidinopyridine

318 mg (1.54 mmol) *N*,*N*′-dicyclohexylcarbodiimide (DCC)

135 mg (0.588 mmol, 0.4fold excess) 2-acryloyloxyethyl glutaric acid monoester **(5)**

9 mg (0.0588 mmol) 4-pyrrolidinopyridine

122 mg (0.588 mmol) *N*,*N*′-dicyclohexylcarbodiimide (DCC)

^{1}H NMR (200 MHz, $CDCl_3$): δ = 7.46–7.34 (m, 4H, aromat. j, k), 7.13–7.09 (d, 2H, aromat. l), 6.92–6.89 (d, 2H, aromat. m), 6.55–6.27 (d, 0.25H, s), 6.18–6.05 (m, 0.25H, r), 5.86–5.81 (d, 0.25H, t), 4.45–4.22 (m, 1.75H, e + n), 3.92–3.27 (s, 2H, d), 2.68–2.45 (2m, 1.5H, o + p, q), 2.3–2.03 (m, 0.75H, f), 1.96–1.26 (m, 19.5H, c + g), 1.13–1.09 (d, 2.25H, i), 1.05–0.85 (t, 2.25H, h), 0.48 (s, 2H, b), 0.35–0 (m, 12H, a).

Yield: 55% of theory.

$\overline{M}_n$ = 7800 g/mol, $\overline{M}_w$ = 12100 g/mol.

$[\alpha]_D^{21}$ = (–1.307)°, c = 0.0145 g/ml $CHCl_3$.

IR (films on NaCl) for **P2**–**P4**: 2962, 2924, 2876, 2854 (C—H valence), 1764 (C=O), 1608, 1498, 1466, 1290, 1260 (Si—C), 1208, 1168, 1096, 1022, 804 cm^{-1}.

2.2.6 Polymer **P5**

^{1}H NMR (200 MHz, $CDCl_3$): δ = 8.59–8.49 (d, 1H, aromat. H_2), 8.30–8.26 (d, 1H, aromat. H_6), 7.56–7.44 (2d, 4H, aromat. $H_{2'}$, $H_{6'}$, $H_{2''}$, $H_{6''}$), 7.22–7.1 (m, 3H, aromat. $H_{3''}$, $H_{5''}$, H_5), 6.94–6.91 (d, 2H, aromat. $H_{3'}$, $H_{5'}$), 4.67–4.6 (m, 1H, C*H—CH_3), 4.01–3.94 (s, 2H, CH_2—O), 1.77–1.25 (m, 31H, C*H—CH_3 und CH_2), 0.86–0.83 (t, 3H, CH_2—CH_3), 0.49–0.35 (s, 2H, Si—CH_2), 0.13–0 (m, 12H, Si—CH_3).

IR (film on NaCl): 2958, 2924, 2854 (C—H valence), 1736 (C=O valence), 1616, 1536, 1498, 1468, 1350, 1284, 1260, 1212, 1168, 1092, 1026, 912, 838, 804, 754 cm^{-1}.

Yield: 59% of theory.

$\overline{M}_n$ = 7500 g/mol, $\overline{M}_w$ = 10500 g/mol.

$[\alpha]_D^{21}$ = (+2.31)°, c = 0.019 g/ml in $CHCl_3$.

^{1}H NMR spectra of polymers **P6**–**P8** are interpreted with the assignment of the H atoms shown in Fig. 2.

2.2.7 Polymer **P6**

(x:y) = (0.95:0.05) quantities used:

890 mg (1.75 mmol) OH-functionalized polysiloxane **(3)**

671 mg (2.275 mmol, 1.3fold excess) 3-nitro-4-(1-(S)-methylheptyloxy)benzoic acid **(6)**

34 mg (0.2275 mmol) 4-pyrrolidinopyridine

470 mg (2.275 mmol) *N*,*N*′-dicyclohexlcarbodiimide (DCC)

205 mg (0.7 mmol, 0.4fold excess) 4-(6-(acryloyloxy-hexyloxy)-benzoic acid **(7)**

10.5 mg (0.07 mmol) 4-pyrrolidinopyridine

145 mg (0.7 mmol) *N*,*N*′-dicyclohexlcarbodiimide (DCC)

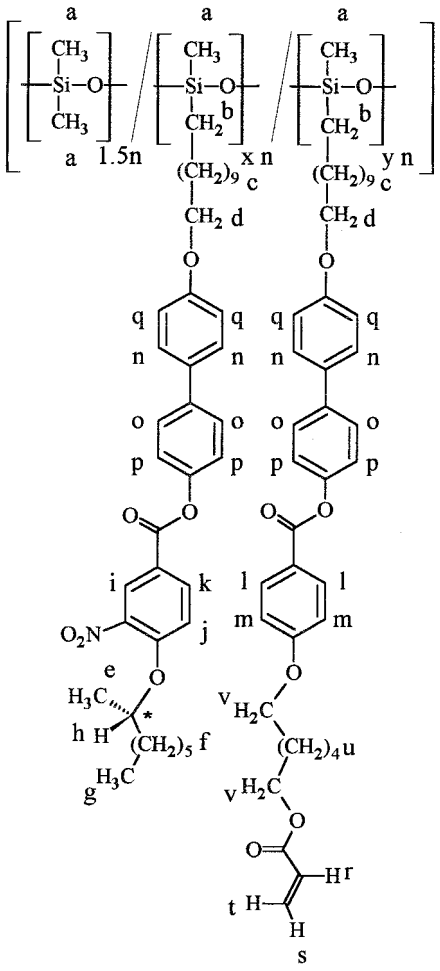

Fig. 2. Molecular structure of terpolymers **P5**–**P8** with assignment of H-atoms

^{1}H NMR (200 MHz, $CDCl_3$): δ = 8.58 (s, 0.95H, aromat. i), 8.29–8.25 (d, 0.95H, aromat. k), 8.14–8.10 (m, 0.1H, aromat. l), 7.52–7.44 (m, 4H, aromat. n + o), 7.21–7.1 (m, 2.95H, aromat. p + j), 6.94–6.9 (m, 2.1H, aromat. q + m), 6.43–6.34 (d, 0.05H, t), 6.17–6.03 (m, 0.05H, r), 5.82–5.77 (d, 0.05H, s), 4.66–4.60 (s, 0.95H, e), 4.24–4.16 (t, 0.2H, v), 4.16–3.94 (s, 2H, d), 1.9–1.10 (m, 30.75H, h + u + f + c), 0.86 (t, 2.85H, g), 0.49 (s, 2H, b), 0.35–0 (m, 12H, a).

Yield: 69% of theory.

$\overline{M}_n$ = 8800 g/mol, $\overline{M}_w$ = 11800 g/mol.

$[\alpha]_D^{21}$ = (+3.517)°, c = 0.0143 g/ml in $CHCl_3$.

2.2.8 Polymer **P7**

(x:y) = (0.85:0.15) quantities used:

950 mg (1.93 mmol) OH-functionalized polysiloxane **(3)**

655 mg (2.22 mmol, 1.15fold excess) 3-nitro-4-(1-(S)-methylheptyloxy)benzoic acid **(6)** 33 mg (0.22 mmol) 4-pyrrolidinopyridine

458 mg (2.22 mmol) *N*,*N*′-dicyclohexylcarbodiimide (DCC)

225 mg (0.772 mmol, 0.4fold excess) 4-(6-acryloyloxy-hexyloxy)benzoic acid **(7)**

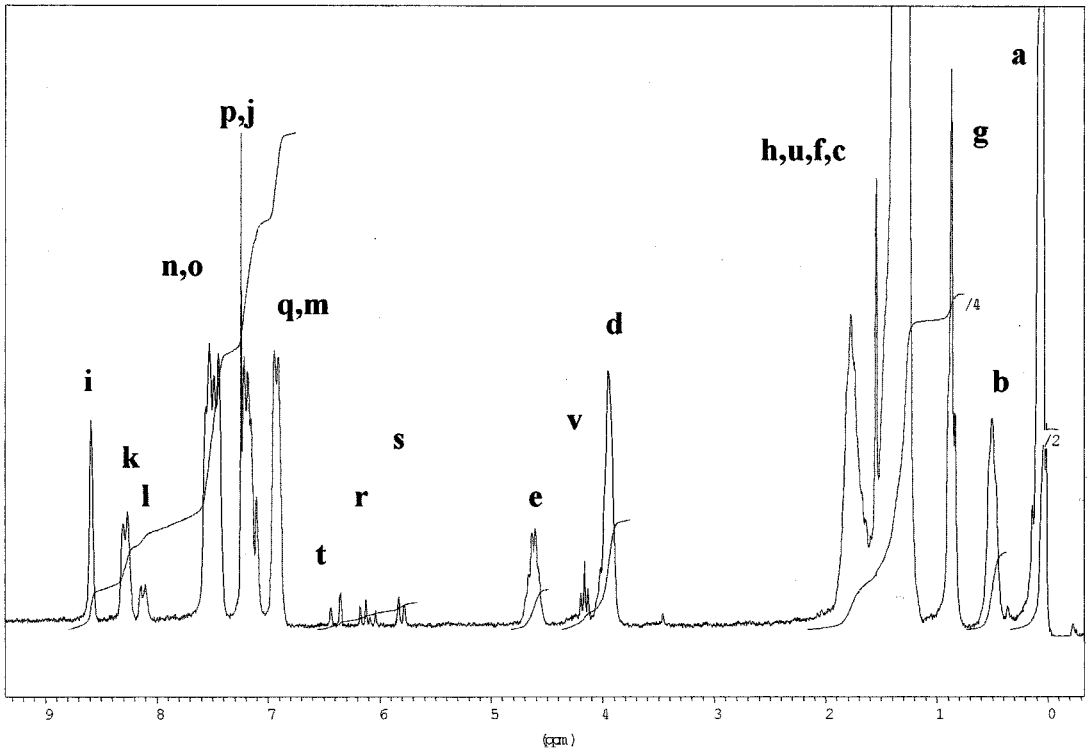

Fig. 3. ^{1}H NMR spectrum (200 MHz, $CDCl_3$) of the crosslinkable terpolymer **P6**. The letters refer to Fig. 2

11.5 mg (0.077 mmol) 4-pyrrolidinopyridine

160 mg (0.772 mmol) *N*,*N*′-dicyclohexylcarbodiimide (DCC)

Fig. 3 shows the ^{1}H NMR spectrum of polymer **P7**.

^{1}H NMR (200 MHz, $CDCl_3$): δ = 8.58 (s, 0.85H, aromat. i), 8.30–8.26 (d, 0.85H, aromat. k), 8.13–8.10 (m, 0.3H, aromat. l), 7.55–7.44 (m, 4H, aromat. n + o), 7.21–7.1 (m, 2.85H, aromat. p + j), 6.94–6.91 (m, 2.3H, aromat. q + m), 6.43–6.34 (d, 0.15H, t), 6.17–6.03 (m, 0.15H, r), 5.82–5.77 (d, 0.15H, s), 4.60 (s, 0.85H, e), 4.24–4.19 (t, 0.6H, v), 4.16–3.94 (s, 2H, d), 1.9–1.10 (m, 30.25H, h + u + f + c), 0.86 (t, 2.55H, g), 0.49 (s, 2H, b), 0.35–0 (m, 12H, a).

Yield: 82% of theory.

$\overline{M}_n$ = 9700 g/mol, $\overline{M}_w$ = 11800 g/mol.

$[\alpha]_D^{21}$ = (+3.842)°, *c* = 0.019 g/ml $CHCl_3$.

2.2.9 Polymer **P8**

(*x*:*y*) = (0.75:0.25) quantities used:

1 g (1.96 mmol) OH-functionalized polysiloxane **(3)**

608 mg (2.06 mmol, 1.05fold excess) 3-nitro-4(-1-(S)-methylheptyloxy)benzoic acid **(6)** 30.5 mg (0.206 mmol) 4-pyrrolidinopyridine

425 mg (2.06 mmol) *N*,*N*′-dicyclohexylcarbodiimide (DCC)

229 mg (0.784 mmol, 0.4fold excess) 4-(6-acryloyloxy-hexyloxy)-benzoic acid **(7)**

11.5 mg (0.078 mmol) 4-pyrrolidino-pyridine

162 mg (0.784 mmol) *N*,*N*′-dicyclohexylcarbodiimide (DCC)

^{1}H NMR (200 MHz, $CDCl_3$): δ = 8.58 (s, 0.75H, aromat. i), 8.26–8.24 (d, 0.75H, aromat. k), 8.13–8.10 (m, 0.5H, aromat. l), 7.52–7.44 (m, 4H, aromat. n + o), 7.21–7.1 (m, 2.75H, aromat. p + j), 6.91 (m, 2.5H, aromat. q + m), 6.43–6.34 (d, 0.25H, t), 6.17–6.03 (m, 0.25H, r), 5.82–5.77 (d, 0.25H, s), 4.60–4.42 (s, 0.75H, e), 4.24–4.19 (t, 1H, v), 4.16–3.93 (s, 2H, d), 1.9–1.10 (m, 29.75H, h + u + f + c), 0.86 (t, 2.25H, g), 0.49 (s, 2H, b), 0.35–0 (m, 12H, a).

Yield: 71% of theory.

$\overline{M}_n$ = 8500 g/mol, $\overline{M}_w$ = 11500 g/mol.

$[\alpha]_D^{21}$ = (+3.030)°, *c* = 0.019 g/ml in $CHCl_3$.

IR (films on NaCl) for **P6**–**P8**: = 2958, 2924, 2854 (C—H valence), 1736 (C═O), 1616, 1570, 1536, 1500, 1468, 1380, 1350, 1284, 1260 (Si—C), 1212, 1168, 1094, 1028, 836, 806, 754 cm^{-1}.

2.3 Physical methods and instrumental equipment

^{1}H- and ^{13}C NMR spectroscopy were recorded using a 200 MHz Bruker AC 200 spectrometer or a 400 MHz Bruker Aspect 3000 spectrometer (university of Mainz). IR-spectra were recorded using a Jasco IR-Report 100 spectrometer or a Bruker IFS 48 FT-IR-spectrometer. GPC measurements were performed using a Waters Liquid Chromatograph (with UV-detector) with a column combination of 10^3 Å (ultrastyrgel) and 10^4 Å (PL-gel). Specific optical rotation was measured using a Perkin-Elmer MC-241 polarimeter (wavelength 589 nm).

The characterization of the LC phases, the ferroelectric characterization[14, 15] and the preparation of the ferroelectric

elastomers was done as described in the preceeding paper[6]. The switching times were determined as time between U_{min} (t) and U_{max} (t) transition change (between 0% and 100% transmission) using the photo-voltage of the photodiode.

3. Results and discussion

3.1 Mesophase behaviour of polymers **P1**–**P8**

Identification of the liquid crystalline phases and determination of the phase transition temperatures revealed the results shown in Tab. 1 and Tab. 2. The two chiral mesogens lead to the formation of smectic-C* phases and high-temperature smectic-A phases in the polymeric systems as expected. The room temperature phase is a highly ordered, almost crystalline and yet unidentified smectic phase, called smectic-X phase. In contrast to the polymers with two mesogenic cores (**P1**–**P4**) the polymers with three mesogenic cores (**P5**–**P8**) show higher phase transition temperatures and a distinct glass transition temperature in the first DSC heating run.

It is obvious that the crosslinkable systems **P2**–**P4** and **P6**–**P8** exhibit the same phase sequence as the synthesized reference copolymers **P1** and **P5**. Whereas all phase transition temperatures in the systems with two mesogenic cores – especially in the crosslinkable systems **P2**–**P4** – stay nearly constant and are independent from the increasing amount of crosslinkable mesogen in the terpolymers, a completely different phase behaviour is observed for the systems containing three aromatic cores (**P5**–**P8**). The smectic-X-smectic-C* phase transition is influenced only slightly by an increasing substitution of chiral by crosslinkable mesogens in polymers **P5**–**P8**. The Curie temperatures (transition smectic-C* to smectic-A) and the clearing points however are shifted to higher temperatures with the result that the smectic-C* phase is widened and therefore stabilized in these systems.

3.2 Ferroelectric characterization of the uncrosslinked polymers **P1**–**P8**

Starting from the Curie temperature T_C the tilt angle of a ferroelectric polymer with a second order smectic-C* smectic-A phase transition increases with decreasing temperature in the smectic-C* phase. The spontaneous polarization increases, too, showing about the same temperature dependence as the tilt angle. Fig. 4 shows the spontaneous polarizations of polymers **P1**–**P4** (with increasing amount of crosslinkable mesogens) as function of the negative reduced temperature ($T-T_C$). Copolysiloxane **P1** shows a spontaneous polarization of 150 nC/cm^2 in saturation. In the terpolysiloxanes **P2**–**P4** 5–25 mol-% chiral mesogens are exchanged for crosslinkable mesogens. As the dipole concentration is reduced in the systems the P_S-values decrease, too, following a non-linear trend as can be followed in Fig. 4. Whereas the spontaneous polarization is 105 nC/cm^2 for terpolymer **P2**, it decreases to 71 nC/cm^2 for terpolymer **P3** and finally drops to 56 nC/cm^2 for terpolymer **P4**.

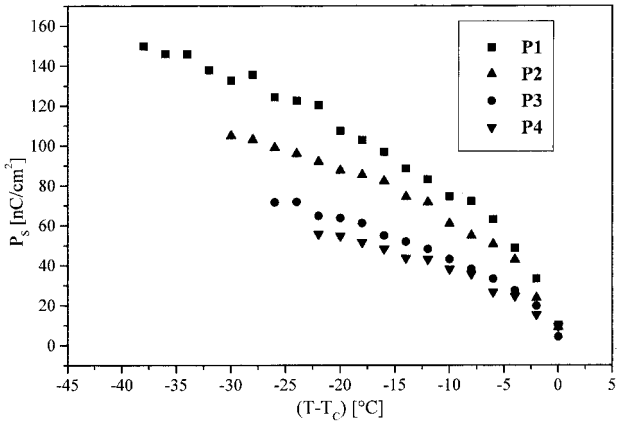

Fig. 4. Temperature dependence of the spontaneous polarizations of **P1**–**P4**

The temperature dependent ferroelectric switching times are plotted single-logarithmically against the negative reduced temperatures in Fig. 5a. The switching times increase with decreasing temperature as the viscosity rises. Terpolymer **P4** reveals almost the same switching times as terpolymer **P3**. Comparing polymer **P1** and **P2** the switching times of **P1** have to be multiplied by a factor of 2 to achieve the times of **P2** over the whole temperature range of the smectic-C* phase. Terpolymers **P3** and **P4** show the 12 fold, respectively the 14.5 fold switching times compared to **P1** at 20 °C reduced temperature (T_C-T). As the Curie temperature remains almost constant in the four systems the increases in the switching times from **P1**–**P4** are due to the increasing viscosity in the systems as more crosslinkable – but not yet crosslinked – mesogens are built in. The P_S- and τ-measurements of **P1**–**P4** were performed using the same field strength (200 V/10 μm). As the same chiral mesogen is present the same temperature dependence of the tilt angle is expected for the four systems. A plot of the product ($\tau \cdot P_S$) against the negative reduced temperatures ($T-T_C$) should therefore lead to a magnitude that is proportional to the rotational viscosity γ in the polymers. Fig. 5b shows this plot. An exponential increase of the "rotational viscosity" is observable with a certain trend: with increasing amount of crosslinkable mesogens the "rotational viscosity" increases earlier with decreasing temperature. **P3** and **P4** show almost the same behaviour. The more chiral mesogens are substituted by crosslinkable ones the slower the polymers switch.

The spontaneous polarizations for the polymers **P5**–**P8** are represented in Fig. 6. As the dipole of the chiral mesogen with three aromatic cores and nitro-substitution is increased compared to the biphenyl with chlorine

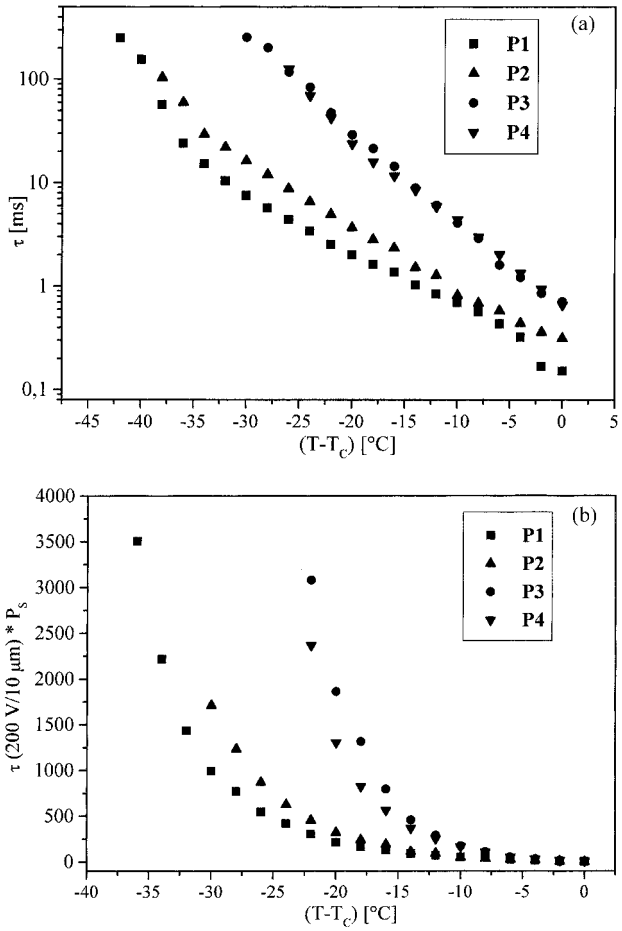

Fig. 5. Temperature dependence of (a) the ferroelectric switching times and (b) the product ($\tau \cdot P_S$) of **P1**–**P4**

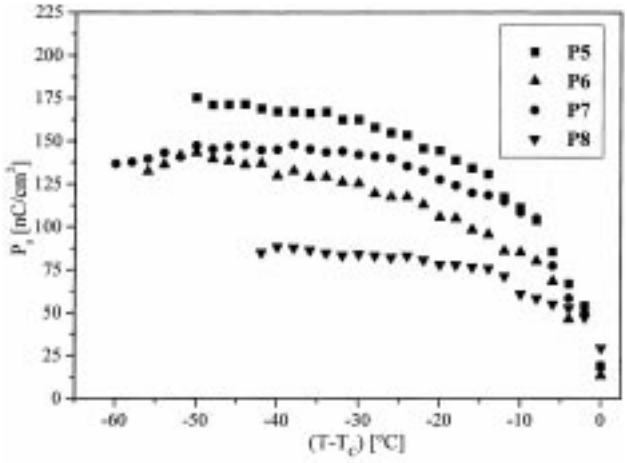

Fig. 6. Temperature dependence of the spontaneous polarizations of **P5**–**P8**

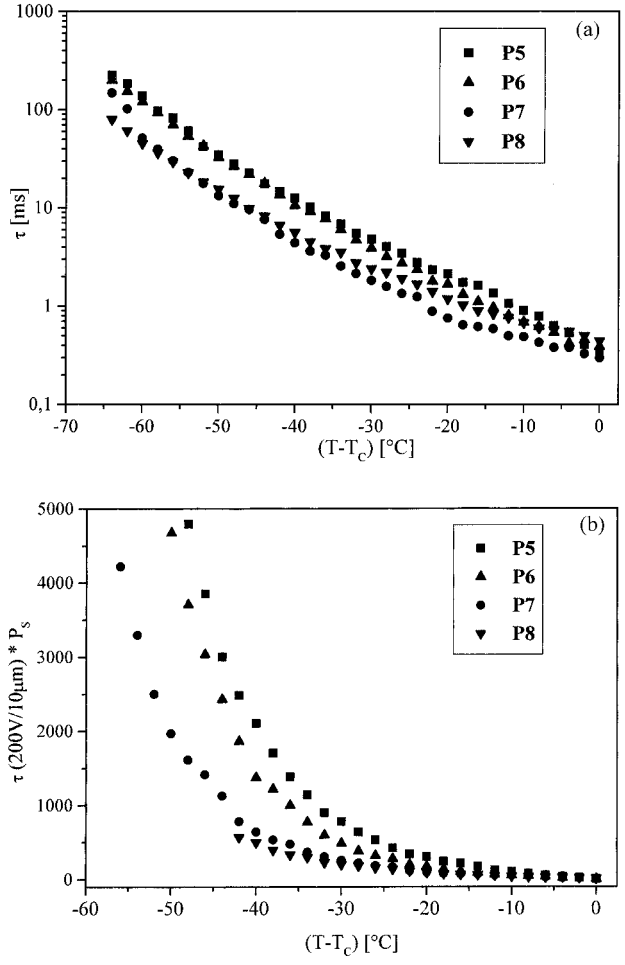

Fig. 7. Temperature dependence of (a) the ferroelectric switching times and (b) the product ($\tau \cdot P_S$) of **P5**–**P8**

dipole, the P_S-values for the polymers increase, too. The same trend as in polymers **P1**–**P4** is observed: The spontaneous polarization decreases with decreasing amount of chiral mesogens. Copolysiloxane **P5** shows a P_S of 175 nC/cm^2. P_S drops to 143 nC/cm^2 in **P6** and 85 nC/cm^2 in **P8**. Polymer **P7** shows a slightly higher P_S than **P6** (147 nC/cm^2). This is probably due to an especially perfect orientation of the LC-cell for **P7**.

The switching times of **P5**–**P8,** however, show a different behaviour compared to the times of **P1**–**P4**. Although the spontaneous polarization decreases from **P5**–**P8** (decreasing torque) the switching times decrease, too. This is presumably due to the increasing Curie temperature (Fig. 7). Therefore measurements performed at the same reduced temperature with regard to the Curie temperature are done at a higher reduced temperature with regard to T_g. Close to the Curie temperature a mixed ferroelectric-electroclinic switching is observed in **P5**–**P8**. Thereby the "original" Curie temperatures of **P5**–**P8** (Tab. 2) are shifted about 4 °C to higher temperatures into the smectic A-phase.

In analogy to Fig. 5b the product ($\tau \cdot P_S$) is plotted against the negative reduced temperature in Fig. 7b. An exponential increase in ($\tau \cdot P_S$) is observed as the temperatures decrease. As the Curie temperatures increase

from **P5**–**P8** the trend of Fig. 6 is reversed following the decreasing viscosity from **P5**–**P8**.

3.3 Influence of the crosslinking on polymers **P2**–**P4**

Going from polymer **P2** to **P4** the amount of mesogens with crosslinkable groups is increased stepwise from 5 mol-% to 25 mol-% (the polymers in ref.[6] have 10 mol-% crosslinkable groups). The influence of the crosslinking density on the resulting networks is studied in detail using these systems. Since all crosslinkable polymers prefer an inter-layer crosslinking, a stabilization of a polar switching state is expected. Terpolymer **P2** with the lowest content of acrylate groups (5 mol-%) shows a lowering of the Curie temperature from 77 °C to 73/74 °C due to the addition of 1 wt.-% photo-initiator (Tab. 1).

The switching times have to be multiplied with a factor 1.5 from pure polymer **P2** to the **P2**/initiator mixture (Fig. 8). After crosslinking (10 °C reduced temperature) the viscosity in the "crosslinked" polymer **P2** (further called elastomer **E2**) increases but a stabilization of one switching state was not observed as proven in two independent experiments. The switching times in elastomer **E2** are increased by a factor of 7 compared to the uncrosslinked **P2**/initiator mixture (Fig. 8). The optical ferroelectric hysteresis is broadened due to the increased viscosity in elastomer **E2**, but there is no shift of the hysteresis indicating a stable polar state. To understand these results the "crosslinked" polymer **P2** was investigated in more detail. It dissolves completely. Obviously the crosslinking reaction only leads to branching and microgel formation and not to a real three dimensional network for **E2**.

An increase in the content of crosslinkable groups to 15 mol-% and 25 mol-%, as realized in polymers **P3** and **P4**, leads to an increase in the crosslinking density in the resulting elastomers and to real insoluble networks. Both elastomers show, after UV-irradiation, a successful stabilization of one ferroelectric switching state but a complete bistable switching is no longer observable in the smectic-C* phase. Fig. 9 a shows the oscilloscope traces of the optical signal for elastomer **E3** in dependence of the applied driving-voltage (200–800 V(pp) triangular wave). The crosslinking density in **E3** is obviously so high that very high voltages (more than 800 V(pp)/10 μm) are necessary to reach the second switching state. Such high voltages were not accessible and would have probably lead to a dielectric breakdown of the sample. The optical signal shows an electroclinic behaviour at low voltages and a transmission change with a narrow, but highly shifted hysteresis at high voltages and low frequencies (Fig. 9b). The elastomers of the preceeding paper[6] contained 10 mol-% of crosslinkable groups and were made from polysiloxanes with a higher degree of polymerization. They combined therefore, network formation with a ferroelectric switching.

Elastomer **E4** reveals no ferroelectric switching in the smectic-C* phase even at very high field strengths of the applied voltage (up to 900 V(pp)/10 μm). The optical signal stays electroclinic due to the high crosslinking density in this system. Obviously the network density is too high, so the product ($P_S \cdot E$) is too low to achieve a deformation of the network. There is no change of texture observable due to the crosslinking reaction. As the original book-

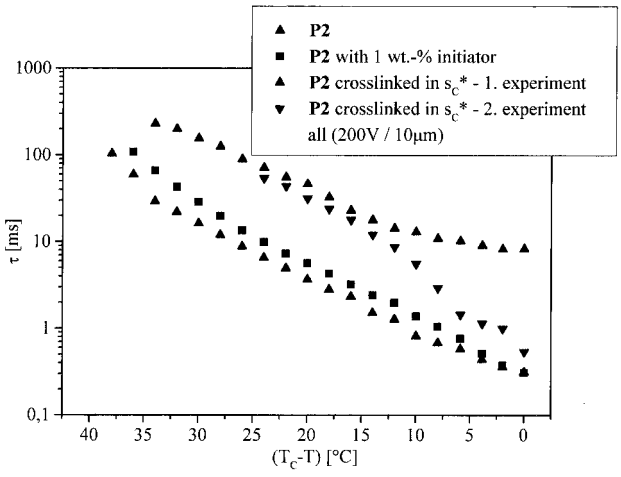

Fig. 8. Ferroelectric switching times of pure polymer **P2**, **P2**/initiator mixture before crosslinking and the elastomer **E2** (τ determined as average of rise- and decay-time)

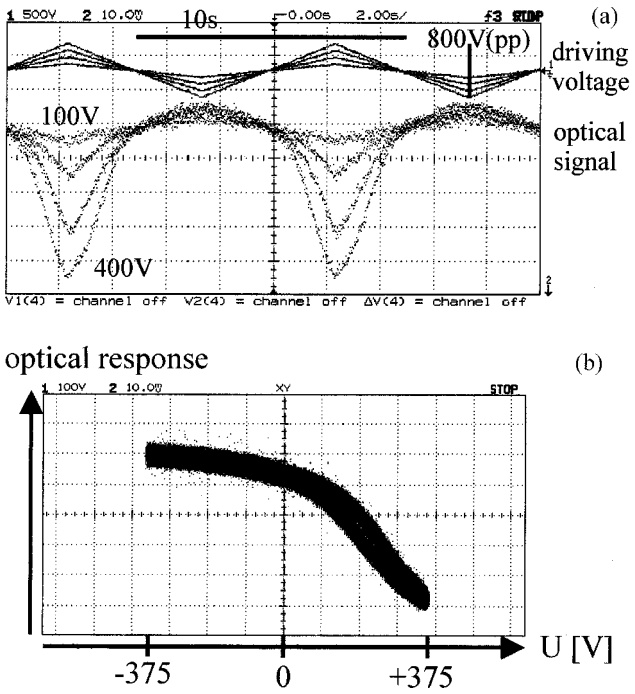

Fig. 9. (a). Oscilloscope traces of the optical signal of elastomer **E3** in dependence of the applied driving voltage, U = 200–800 V(pp) applied triangular wave, f = 0.1 Hz, T = 64 °C and (b) resulting ferroelectric hysteresis (U = 750 V (pp))

shelf-geometry is not changed the tilt of the mesogens at 10 °C reduced temperature should therefore be fixed and a permanent macroscopic polarization is expected for **E4**.

3.4 Influence of the crosslinking on polymers **P6**–**P8**

A variation of the chemical structure of the chiral mesogen from two to three aromatic cores and a change in the chiral tail resulted in polymers with higher spontaneous polarizations. Simultaneously the crosslinkable mesogen was lengthened, too, to fit the molecular structure.

Terpolymer **P6** contains 5 mol-% crosslinkable mesogens. An addition of 1 wt.-% photo-initiator lowers T_C from 115 °C to 110 °C in the **P6**/initiator mixture. A temperature of 80 °C (30 °C reduced temperature) was chosen as crosslinking temperature. At this temperature the plateau-value of the optical tilt angle of 35° (±1°) was reached as determined by polarization microscopy. The higher reduced temperature (but comparable absolute temperature) for crosslinking – compared to the systems **P2**–**P4** – was chosen with regard to the polymerization kinetics of the acrylate group during the radical photocrosslinking. Below 90 °C an increasing polymerization rate with increasing temperature is found. In the temperature range of 90–145 °C side reactions take place lowering the polymerization rate and above 145 °C the rate is lowered to a high extent due to a depolymerization of the previously formed polymer chains[16].

Photo-crosslinking of **P6** is performed by UV-irradiation of the oriented **P6**/initiator mixture in a LC cell with an applied bias field of 100 V/10 μm at 80 °C. In analogy to the slightly crosslinked elastomer **E2** with 5 mol-% crosslinkable groups, a stabilization of one ferroelectric switching state is not observed in **E6**. The ferroelectric hysteresis for **E6** is merely broadened compared to the uncrosslinked **P6**/initiator mixture. As for polymer **P2** no three dimensional network is formed by the crosslinking reaction. The switching times of the **P6**/initiator mixture are increased by a factor of 1.5 compared to the pure polymer **P6** (Fig. 10) due to the lowering of T_C. After irradiation the switching times are increased by a factor of 10. The **E6** elastomer with three aromatic cores shows – in comparison to elastomer **E2** with two aromatic cores – a stronger increase in the switching times. This result is most likely explained by a higher sensitivity of the longer mesogen with regard to the network structures formed.

Terpolymer **P7** (with 15 mol-% crosslinkable mesogens) shows an asymmetric ferroelectric switching (Fig. 11) after irradiation (80 °C, with a bias field of 100 V/10 μm). A stabilization of one switching state was successful. Obviously the higher ferroelectric polarization makes it possible to reach the second (destabilized) switching state at lower voltages.

Fig. 12 a and b show the optical hystereses for polymer **P8** before and after crosslinking with an applied d.c.-field

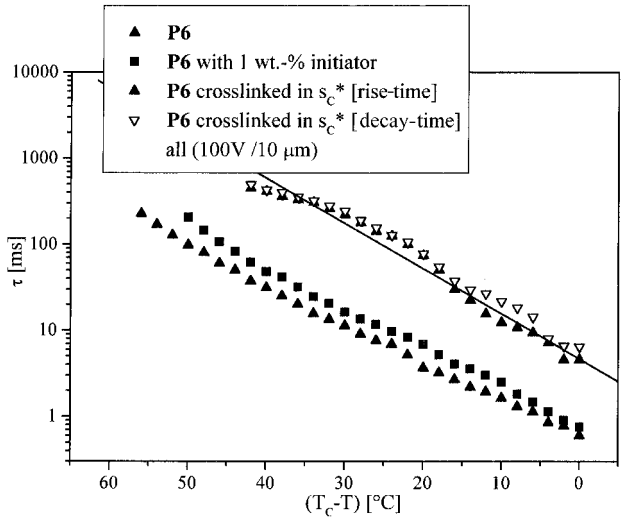

Fig. 10. Temperature-dependent switching times of **P6**, the **P6**/initiator mixture and elastomer **E6** (rise- and decay-times)

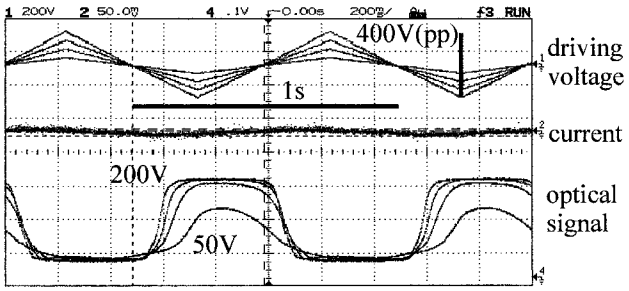

Fig. 11. Oscilloscope traces of the optical signal and the current of elastomer **E7** in dependence of the applied driving-voltage, U = 100–400 V(pp) applied triangular wave, f = 1 Hz, T = 80 °C (smectic-C*)

(100 V/10 μm) in the smectic-C* phase (at 80 °C). The highest crosslinking density in the elastomeric systems **E6–E8** is reached in elastomer **E8**. Here the ferroelectric hysteresis shows the highest asymmetry and the strongest shift. As the viscosity in elastomer **E8** was strongly increased, the frequency had to be lowered to record the hysteresis.

The two switching states of **P8** in the smectic-C* phase are illustrated before and after UV irradiation in Fig. 13. A decrease in the optical contrast is observed after crosslinking. The cracks in Fig. 13 c and d occur as a result of continuous switching. They are presumably a result of the mechanical stress within the network, as the mesogens are switched to the unfavourable switching state.

The switching times for elastomer **E7** and **E8** are shown in Fig. 14. There is a difference between rise- and decay-time for **E7** of almost a factor 3. For **E8** rise- and decay-time differ by a factor of 5. The difference of the rise- and decay-time is a further indication of the strength of the crosslinking density in the elastomers. A higher

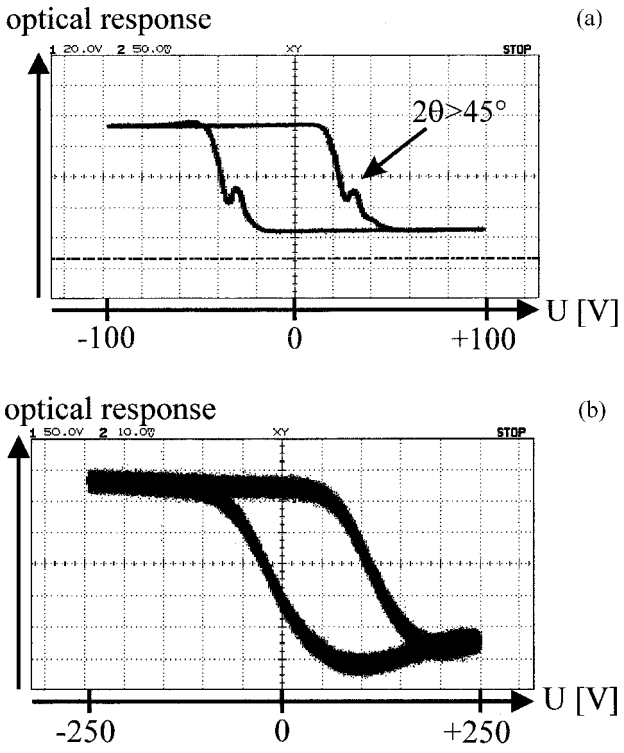

Fig. 12. Ferroelectric optical hysteresis of (a) polymer **P8** before crosslinking, U = 200 V, f = 4 Hz, T = 80 °C and (b) of elastomer **E8** after crosslinking, U = 500 V, f = 0.5 Hz, T = 80 °C

preference of one switching state leads to an increase in the electric field that is necessary to switch *against* the mechanic field of the network and simultaneously to a decrease of the electric field necessary to switch *with* the mechanic field back into the stabilized state.

4. Conclusion

Polysiloxanes with mesogens consisting of two mesogenic cores show a small influence of the phase transition temperatures on the content of crosslinkable mesogens. Systems with mesogens containing three aromatic cores reveal a broadening and a stabilization of the smectic-C* phase due to an increase in Curie temperature and clearing temperature with increasing amount of crosslinkable mesogen. Due to the decreasing dipole concentration the spontaneous polarization decreases with increasing amount of crosslinkable mesogens for both polymer series.

Polymers with the smallest amount of crosslinkable side-groups could not be used to prepare elastomers with a real three-dimensional network. Polymers with higher amounts form real networks. As for as the polysiloxanes with mesogens of two mesogenic cores are concerned, a photo-crosslinking leads to polar elastomers that can, however, not be switched completely due to a high crosslinking density and a too low spontaneous polarization.

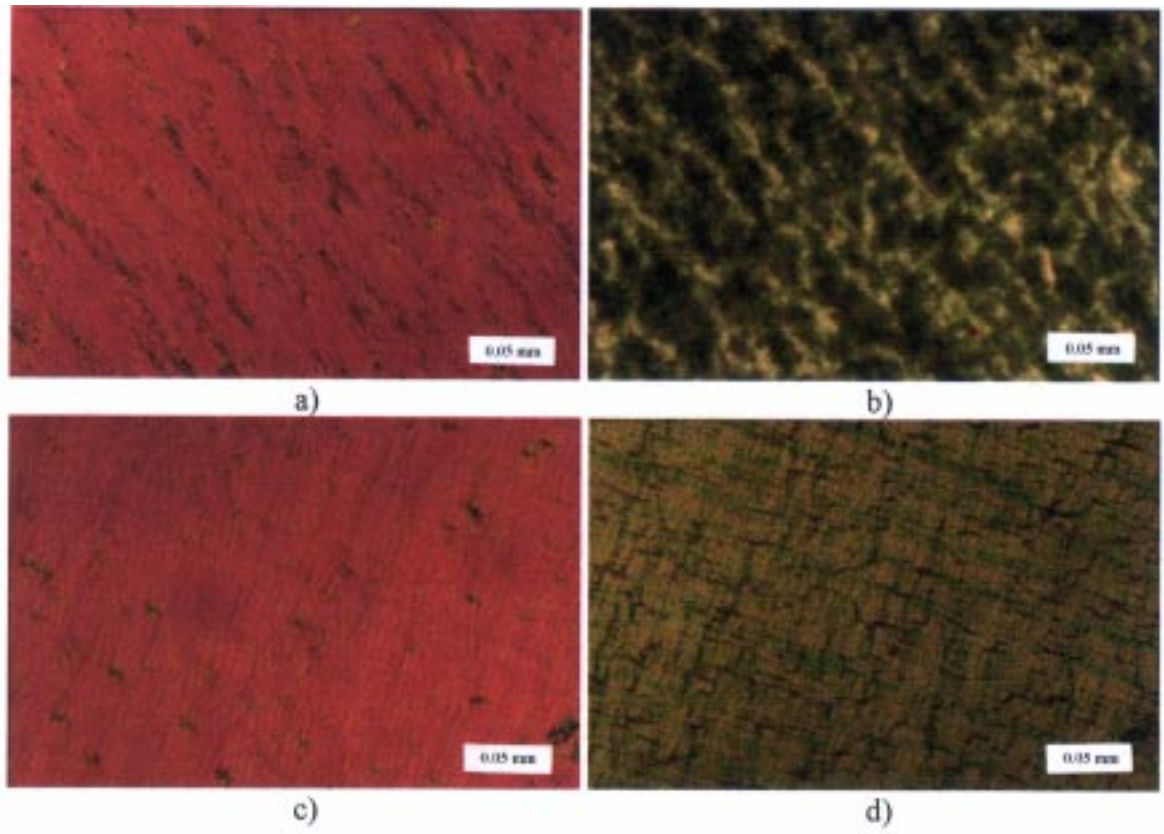

Fig. 13. Polarizing micrographs of the two bistable switching states of polymer **P8** at T = 80 °C; a, b: before crosslinking, c, d: after crosslinking

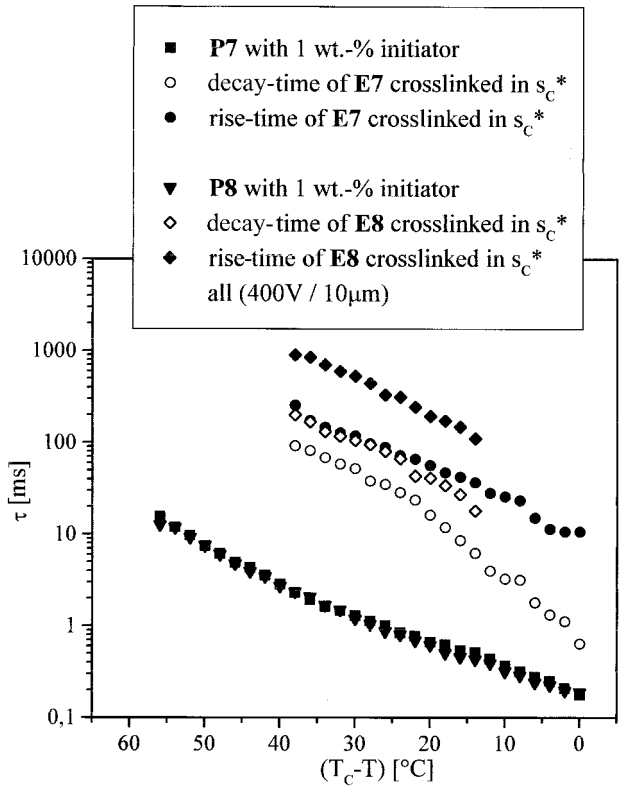

Fig. 14. Temperature dependence of the ferroelectric switching times of polymers **P7** and **P8** with admixture of 1 wt.-% photoinitiator and rise- and decay-times in elastomers **E7** and **E8**

Elastomers with three aromatic cores (the larger mesogens) are more sensitive to network formation regarding the switching times (kinetic aspects). As they possess a larger ferroelectric polarization, they can, however, be switched completely if enough time is available. This happens because the torque ($P_S \cdot E$) acting on the mesogens is – this time – large enough to overcome the elastic field of the polymer network at accessible external voltages.

Acknowledgement: The authors are grateful to the Consortium für Elektrochemische Industrie for supplying the hydrosilylation catalyst. We thank the DFG for financial support.

[1] R. Zentel, *Angew. Chem., Adv. Mater.* **101**, 1437 (1989)
[2] W. Gleim, H. Finkelmann, in: "*Side Chain Liquid Crystal Polymers*", C. B. Mc Ardle (Ed.), Blackie and Son Ltd., Glasgow 1989, p. 287
[3] F. J. Davis, *J. Mater. Chem.* **3**, 551 (1993)
[4] M. Brehmer, R. Zentel, G. Wagenblast, K. Siemensmeyer, *Macromol. Chem. Phys.* **195**, 1891 (1994)
[5] M. Brehmer, R. Zentel, F. Gießelmann, R. Germer, P. Zugenmaier, *Liq. Cryst.* **21**, 589 (1996)
[6] E. Gebhard, R. Zentel, *Macromol. Chem. Phys.* **201**, 902 (2000)
[7] H. Poths, R. Zentel, *Liq. Cryst.* **16**, 749 (1994)
[8] A. Hassner, V. Alexanian, *Tetrahedron Lett.* **46**, 4475, (1978)
[9] B. Koppenhöfer, V. Schurig, *Org. Synth.* **66**, 151 (1988)
[10] H. Kapitza, R. Zentel, *Macromol. Chem.* **192**, 1859 (1991)
[11] M. Portugall, H. Ringsdorf, R. Zentel, *Makromol. Chem.* **183**, 2311 (1982)
[12] H. Poths, E. Wischerhoff, R. Zentel, A. Schönfeld, G. Henn, F. Kremer, *Liq. Cryst.* **18**, 811 (1995)
[13] A. Kocot, R. Wrzalik, J. K. Vij, M. Brehmer, R. Zentel, *Phys. Rev. B* **50**, 16346 (1994)
[14] Ph. Martinot-Lagarde, *J. Phys. (France)* **38**, L17 (1977)
[15] K. Miyasato, S. Abe, H. Takezoe, A. Fukuda, E. Kuze, *Jpn. J. Appl. Phys.* **22**, L611 (1983)
[16] D. J. Broer, G. N. Mol, G. Challa, *Polymer* **32**, 690 (1991)